Journal Pre-proof
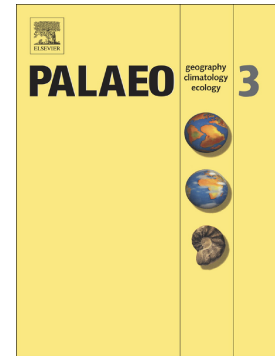
Morphological evolution of the cave bear (Ursus spelaeus) mandibular molars: coordinated size and shape changes through the Scladina Cave chronostratigraphy

Daniel Charters, Richard P. Brown, Grégory Abrams, Dominique Bonjean, Isabelle De Groote, Carlo Meloro

Please cite this article as: D. Charters, R.P. Brown, G. Abrams, et al., Morphological evolution of the cave bear (Ursus spelaeus) mandibular molars: coordinated size and shape changes through the Scladina Cave chronostratigraphy, *Palaeogeography, Palaeoclimatology, Palaeoecology* (2021), https://doi.org/10.1016/j.palaeo.2021.110787

This is a PDF file of an article that has undergone enhancements after acceptance, such as the addition of a cover page and metadata, and formatting for readability, but it is not yet the definitive version of record. This version will undergo additional copyediting, typesetting and review before it is published in its final form, but we are providing this version to give early visibility of the article. Please note that, during the production process, errors may be discovered which could affect the content, and all legal disclaimers that apply to the journal pertain.

Morphological evolution of the cave bear (*Ursus spelaeus*) mandibular molars: coordinated size and shape changes through the Scladina Cave chronostratigraphy

Daniel Charters [a, *], Richard P. Brown [a], Grégory Abrams [b, c], Dominique Bonjean [b, d], Isabelle De Groote [a, e], Carlo Meloro [a].

[a] Research Centre in Evolutionary Anthropology and Palaeoecology, School of Natural Sciences and Psychology, Liverpool John Moores University, Liverpool, UK

[b] Scladina Cave Archaeological Centre, Rue Fond des Vaux 339D, 5300, Andenne, Belgium

[c] Faculty of Archaeology, Leiden University, Postbus 9514, 2300 RA, Leiden, Netherlands

[d] Department of Prehistory, University of Liège, Place du 20 Août, 7, 4000, Liège, Belgium

[e] Department of Archaeology, Ghent University, Sint-Pietersnieuwstraat 35, UFO 9000 Gent, Belgium

*Corresponding author: Daniel Charters   D.J.Charters@2019.Ljmu.ac.uk

Abstract

Out of all extinct megafaunal mammals of the Quaternary, the cave bear *Ursus spelaeus* is one of the best represented in the fossil record. This species has been found to exhibit skeletal morphological adaptations when exploiting varied environmental niches, be that spatially or temporally. Here, we employ geometric morphometrics and phenotypic trajectory analysis to explore temporal morphological changes across the entire lower molar tooth row from the infilling of Scladina Cave, Belgium. We show that molar tooth size increases from Marine Isotope Stage (MIS) 5 – MIS 3, with cusp position varying temporally in relation to a larger talonid grinding platform in later time periods. Phenotypic trajectory analyses further show similar evolutionary shape trajectories in the first and second molars,

but not in the third molar. Morphological changes related to a larger grinding platform are found in the second and third molars, with the divergent morphological change of M_3 suggesting that this tooth is less constrained and appears much more responsive to environmental changes. The need to cope with harder fibrous plant material present in the palaeoenvironment potentially constrained morphological evolution of the cave bear until its disappearance throughout Europe.

Keywords: Geometric Morphometrics, Habitat Adaptation, Molars, Phenotypic Trajectory Analysis, Quaternary.

1. Introduction

One of the main representatives of Quaternary megafauna is the cave bear (*Ursus spelaeus sensu lato*) that roamed Eurasia before its extinction approaching the last glacial maximum (LGM) around ca. 25 kya (Baryshnikov, 2007; Baca *et al*., 2016). Extensive research over recent years through $\delta^{13}C$, $\delta^{15}N$ isotopic and morphometric analyses of fossil assemblages have indicated that the cave bear was mostly herbivorous or a relatively herbivorous omnivore that predominantly consumed plants and mast (Kurtén, 1968; Bocherens *et al.,* 1997, 1999, 2006, 2014a; Garcia, 2003; Figueirido *et al*., 2009; Peigné *et al*., 2009; Baryshnikov and Puzachenko, 2011; Münzel *et al*., 2011; Bocherens, 2015, 2019; Pérez-Ramos *et al*., 2019; Van Heteren and Figueirido, 2019). However, some aspects of the cave bear evolutionary history are still under debate including: its multiple lineage categorisation (*U. spelaeus, U. ingressus, U. rossicus* and *U. kudarensis* (Baryshnikov and Foronova, 2001; Rabeder *et al.*, 2008, 2010; Knapp *et al.*, 2009; Stiller *et al*., 2014)) and the processes of sub-speciation and adaptation to different habitats (steppe to forest, Baryshnikov and Puzachenko, 2018).

Chronological changes in size have been previously identified from fossil remains of cave bears and other mammals (Seetah *et al.*, 2012), generally characterised by smaller individuals than those groups associated closer to the LGM or another cold climatic period (de Carlis *et al.*, 2005). Here, we look at size and shape changes within the cave bear (*U. spelaeus*) dentition of the Scladina Cave (Belgium) assemblage. Size differences in cave bear assemblages have been associated with climatic variation through time as expected for mammals that obey Bergmann's rule (Bergmann, 1847; Meiri *et al.*, 2004, 2007; Toskan, 2007; Watt *et al.*, 2010; Miracle, 2011; Clauss *et al.*, 2013). However, concurrent views on this relating to mammals and other taxonomic classes are limited (Ashton *et al.*, 2000; Meiri and Dayan, 2003; Meiri *et al.*, 2004; Meiri and Thomas, 2007). Experimental evaluations of mechanisms behind size changes are needed if a rule is to be falsifiable (Watt *et al.*, 2010). One such rule, proposed by Huston and Wolverton (2011), called "the eNPP rule". It is based on food availability and provides an alternative to Bergmann's thermoregulatory hypothesis. Huston and Wolverton's (2011) findings suggest Bergmann's hypothesis of heat conversion has very limited ability to explain latitudinal variation in body size, finding a lack of latitudinal patterns within the topics and a decline in body size above a latitude of 60°. The small cave bear *U. rossicus* found throughout southern Siberia is one such example, living in regions with latitudes of around 60° and possessing a body size much smaller than that of its European counterparts who inhabited regions of much lower latitudes (Baryshnikov and Foronova, 2001).

Additional explanations of intraspecific variation in body size come from the productivity paradox. Recent research utilising a grazing model for present day and LGM large grazers was used to simulate the association between body size variation and primary productivity. Findings suggested a 79-93% reduction in biomass in present day ecosystems compared to those predicted for the LGM with larger body sizes of grazers around the LGM

and a more prolific exploitation of vegetation by large bodied herbivores being observed (Zhu *et al.*, 2018). These arguments surrounding body size variation within mammals raise more questions about the mechanisms behind phenotypic changes. Still, diverse evidence supports the hypothesis that environmental changes stimulated phenotypic adaptations in flora and fauna especially during harsh glacial and interglacial fluctuations of the Quaternary's 2.6-million-year period (Dansgaard *et al.*, 1982; Johnsen *et al.*, 1992; Taboda *et al.*, 2001; Baryshnikov *et al.*, 2003, 2004; Barnosky, 2004; Lister, 2004; Athen *et al.*, 2005; de Carlis *et al.*, 2005; Koch and Barnosky, 2006; Stuart and Lister, 2007; Lorenzen *et al.*, 2011; Rabeder *et al.*, 2011; Böse *et al.*, 2012; Toskan and Bona, 2012; Bocherens *et al.*, 2014b; Rasmussen *et al.*, 2014; Sandom *et al.*, 2014; Stuart 2015; Krajcarz *et al.*, 2016; Robu, 2016; Robu *et al.*, 2018). Most of these phenotypic variations have been detected through fossil studies of dentition (the most commonly used element due to its high rate of preservation), skulls and long bones (Elton, 2006; Huysseune *et al.*, 2009; Meloro *et al.*, 2013; Meloro and Olivera, 2019).

Morphological studies have suggested that cave bears exhibited a potentially rapid response rate to climate change, with their dentition showing environmental and diet driven changes (Kurtén, 1955; Rabeder and Tsoukala, 1990; Mattson, 1998; Rabeder, 1999; Sacco and Van Valkenburgh, 2004; Christiansen, 2007; Baryshnikov and Puzachenko, 2018). The cave bear developed specialized dentition to accentuate grinding functions, an evolutionary trend that included the development of a large masticatory platform across the cheek teeth. This trend diverges from an earlier "cutting" morphology seen in other closely related members of the *Ursus* clade such as *U. arctos* and *U. deningeri* (Grandal-d'Anglade and López-González, 2005; Krause *et al.*, 2008). Additionally, patterns of lower tooth size variation within ursids have been suggested to diverge from what is commonly observed in other mammals. The inhibitory cascade model (IC) has been used in this regard, to

understand variation in molars and the loss of third molars, although ursid species apparently fail to conform to this model generally showing a pattern of $M_1 < M_2 > M_3$ (Kavanagh *et al.*, 2007; Asahara *et al.*, 2016). This suggests that not all lower cheek teeth of cave bears might respond in the same way to environmental changes.

Scladina Cave is of great biological significance due to its Neanderthal remains, abundance of other fossil remains and highly detailed chronostratigraphic infilling (Toussaint et al., 1994; Bonjean, 1995; Pirson, 2007; Abrams et al., 2014; Pirson *et al.*, 2014; Toussaint and Bonjean, eds., 2014). Previous research on cave bears from the Scladina Cave stratigraphic sequence further corroborated findings of tooth size increase towards a temporal sequence. Morphological changes have been identified in the talon of the M^2 (second upper molar) together with the reduction in general size of M^1 (first upper molar) (Charters *et al.*, 2019). These created a more substantial masticatory platform whilst biomechanical performance for effective mastication was efficiently maintained. Furthermore, an association with distinct environmental or climatic niches supported the hypothesis that these changes in upper molariform dentition were adaptive (Baryshnikov *et al.*, 2003, Baryshnikov and Puzachenko, 2018).

Here, we employ geometric morphometrics (GMM, Bookstein, 1991; Adams *et al.*, 2004, 2013) and phenotypic trajectory analysis (PTA; Adams and Collyer, 2009; Collyer and Adams, 2013) to analyse size and shape change in the three lower molar teeth of the cave bears from Scladina Cave. We test the hypothesis that lower molar size and shape will change over the temporal scale of 90 thousand years and assess the conformity of *U. spelaeus* to the IC model. Because size and shape of lower dentition are highly integrated within the Carnivora (Kurtén, 1967; Polly, 2007; Asahara *et al.*, 2016) we hypothesise that the three lower molars should exhibit parallel trajectories in shape changes over time. Baryshnikov and

Puzachenko (2020) have recently provided another view for the cave bear in relation to the inhibitory cascade model with data suggesting a $M_1 \approx M_2 > M_3$ pattern. Although some of the Scladina Cave teeth are isolated and may come from different individuals, we would expect this model to apply also for this sample with M_2 being generally larger than M_1 and M_3 in all temporal sequences. There are no well-defined expected outcomes for shape changes based on the IC model, however based on our previous study (Charters *et al.*, 2019) we do expect molar shape changes over time to exhibit parallel trajectories. This is because the lower molar dentition should maintain its masticatory functionality to allow efficient feeding. So, shape changes of one tooth type over time should be followed by shape changes of the adjacent tooth.

To this aim, we employed PTA which has been previously used to statistically test trajectories from mammalian ontogeny (Terhune *et al.*, 2018; Durão *et al.*, 2019; Mori and Harvati, 2019) to evolutionary trends (Martinez *et al.*, 2018). PTA provides evolutionary trajectories, which have orientation, magnitude and shape attributes and therefore allow detailed insights into variation and divergence within and among stratigraphic contexts (Adams and Collyer, 2009). Due to the environment-associated phenotypic plasticity of dentition found in a diverse array of taxa (Huysseune, 1995), we predicted that correlated phenotypic changes in lower molars should be detectable among cave bear chrono-populations from Scladina.

2. Materials and Methods

2.1 Sites and Specimens

This study is based on 524 lower molars (see Table 1) from *U. spelaeus* pertaining to three separate stratigraphic sedimentary units of Scladina Cave, Belgium ($50^{\circ}29'33''$ N,

5°1'30" E). A complete list of specimens and their stratigraphic association is presented in

Table 1 and in the supplementary data Table S1.

Tooth/Unit	1A	3	4A	Total
M_1	75	67	49	191
M_2	106	70	57	233
M_3	40	27	33	100
Total	221	164	139	524

Table 1. Specimens used for this study of lower first (M_1), second (M_2) and third molars (M_3) with stratigraphic origin: 1A (MIS3), 3 (MIS3 and/or MIS 4) and 4A (MIS 5).

Scladina is the main cave of a small cave complex, linked by the Saint-Paul and Sous-Saint-Paul caves (Bonjean *et al*., 2014; Pirson, 2007; Pirson *et al*., 2008; Figure 1). All dentition presented here is associated with the sedimentary units 4A, 3 and 1A of Scladina spanning from MIS 5 to MIS 3 (4A < 130±20kya, MIS 5; 3 MIS 4 and/or MIS 5; 1A ~38-40 kya, MIS 3) (Pirson *et al*., 2014). The dating of the units was carried out using differing methods on the unit sediment and/or objects associated with the corresponding sedimentary unit (Abrams *et al*., 2010; Bonjean *et al.,* 2011; Pirson *et al*., 2008, 2014). A detailed chronostratigraphic translation of the karstic sedimentary deposits throughout the cave network allows further interpretation and clarification of these dating techniques (Pirson *et al*., 2014) (Figure 1). Dentitions that were heavily worn, containing occlusal fractures (whole, but size/cusp position were affected), fractured or distorted outline or possessed occlusal concretion of minerals were excluded from the study. Occlusal surface photographs were
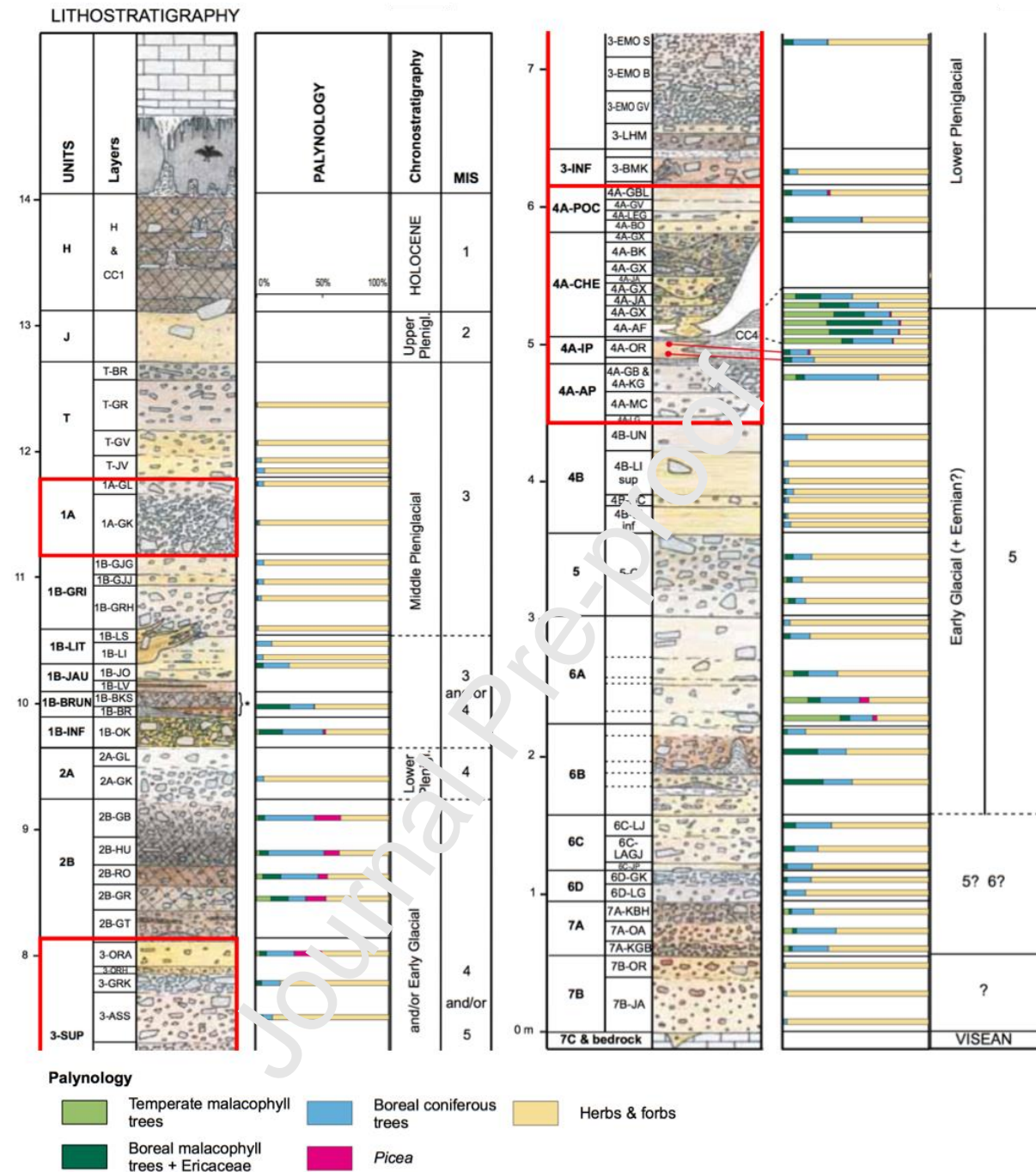
only taken if these characteristics were absent.

Figure 1. The chronostratigraphic sedimentary sequence, related palynology and related Marine Isotope Stages of Scladina Cave (top left to bottom right). Units analysed in this study are highlighted in red boxes (Modified after Pirson *et al*., 2014).

2.2 Landmark Configuration

Images of dental occlusal surfaces were taken using a Nikon D5300 equipped with a Sigma 70-300mm f 4.0-5.6 APO GD Macro lens at a distance of 70 cm. The camera lens was positioned parallel to the occlusal surface of each specimen using a Manfrotto tripod and camera mounted spirit level. Five two-dimensional fixed landmark positions were produced and placed using tpsDIG2 software (version 2.31; Rohlf, 2015) by a single operator (D.C.) to avoid inter-observer error. The landmark configuration was chosen to accurately detail the main molariform cusps concurrent on all three inferior molars (Figure 2 and 3). Several cusps can be detected on these teeth, however here we limited our landmarking to homologous points detectable in all the teeth. This procedure allowed analyses of three different molars within the same morphospace. This approach was introduced by Bastir *et al.*, (2014) who were able to interpret variation within and between thoracic vertebrae of humans. For definitions and configuration of anatomical landmarks see Table 2.
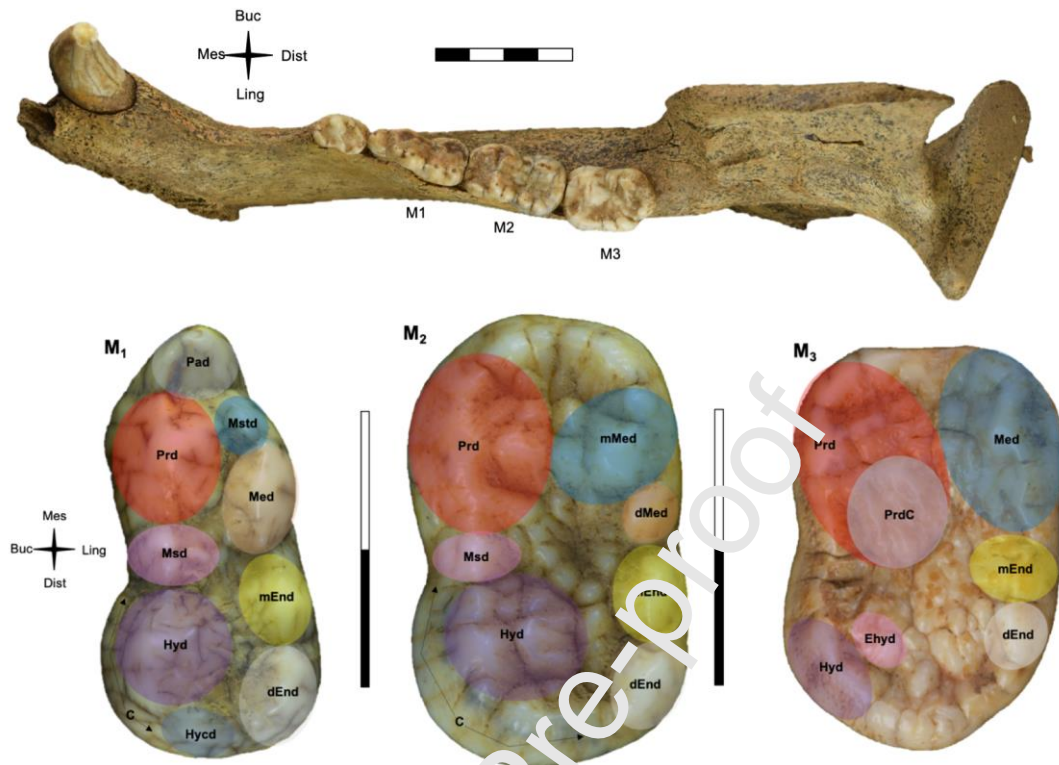
Figure 2. (*above*) Right hemi-mandible (SC-92-503-1) of *U. spelaeus* with dentition in anatomical position. (below, *left to right*) Anatomical nomenclature for M_1, M_2 and M_3. Abbreviations: **Pad** - Paraconid, **Prd** – Protoconid, **Med** – Metaconid, **Hyd** – Hypoconid, **Msd** – Mesoconulid, **Hycd** – Hypoconulid, **dEnd** – Distal Entoconid, **mEnd** – Mesial Entoconid, **Mstd** – Metastylid, **dMed** – Distal Metaconid, **mMed** – Mesial Metaconid, **PrdC** – Protoconid Complex, **Ehyd** Enthypoconid, **C** – Cingulum.
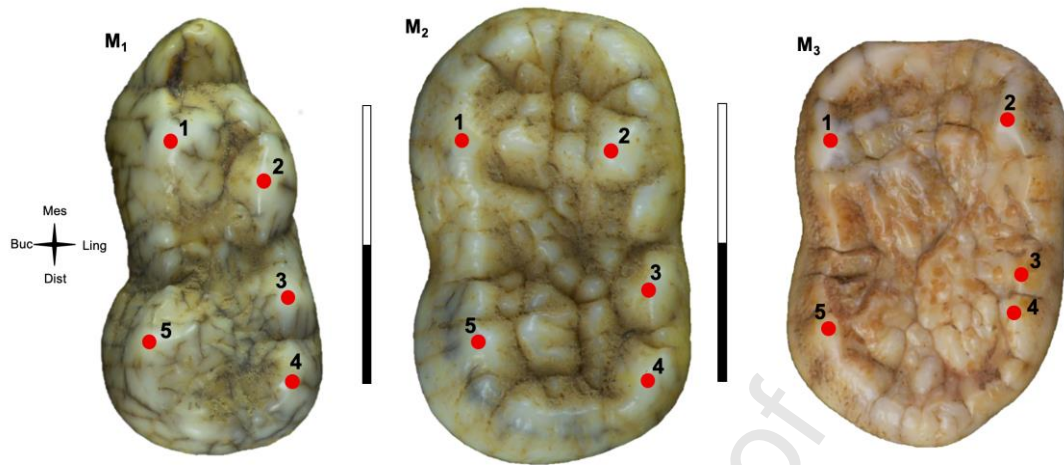
Figure 3. (*left to right*) Landmark configuration for M_1, M_2 and M_3. Refer to Table 2 for definitions.

Landmark	Definition
1	Peak of Protoconid
2	Peak of Metaconid
3	Peak of Mesial Entoconid
4	Peak of Distal Entoconid
5	Peak of Hypoconid

Table 2. Definition and numbering sequence of landmarks for M_1, M_2 and M_3.

2.3 Geometric Morphometrics (GMM) and Phenotypic Trajectory Analysis (PTA).

Initially, a superimposition of 2D landmark coordinates (translation, rotation and scaling) was computed using a Generalised Procrustes Analysis (GPA) for M_1, M_2 and M_3 (first, second and third lower molars) run in the same GPA and separately to produce a new set of coordinates named Procrustes coordinates (Gower, 1975; Rohlf and Slice, 1990). Procrustes coordinates provide a quantitative representation of specimen shape while size information is retained by the natural logarithm of centroid size (LnCS; is the square root of the sum of squared distances between each landmark position and the centroid; Bookstein,

1989; Rohlf, 2000). The natural logarithm of centroid size was used to ensure normality and isotropic distribution of variables that define the shape space. Size differences were first assessed with one-way analyses of variance (ANOVA) on LnCS in R (version 4.1.1) using the packages Geomorph (version 4.0) and RRPP (version 1.0) (Adams and Otarola-Castillo, 2013; Adams and Collyer, 2015, Collyer and Adams, 2018, 2019, 2021; Adams *et al.*, 2021; Baken *et al.*, 2021; R Core Team, 2021) for stratigraphic units modelled as factors. This was succeeded by pairwise tests and visualized by box plots for each tooth type. Procrustes ANOVA was adopted to test the variation within and between molar shape using the R (version 4.1.1) package Geomorph (version 4.0; Adams and Otarola-Castillo, 2013; Adams and Collyer, 2015) on shape variables, accompanied by pairwise permutations (using residual randomisation with 1000 permutations) in RRPP (version 1.0) (Collyer and Adams, 2018, 2019, 2021; Adams *et al.*, 2021; Baken *et al.*, 2021; R Core Team, 2021). We tested the null hypotheses that tooth type, stratigraphical layer (*i.e.*, time) and their interaction accounted for shape variation in the total sample.

Visualisation of shape differences were produced through a Principal Component Analysis (PCA) using R, alongside deformation grids produced in PAST (version 2.17c, Hammer *et al.,* 2001) and mean deformation wireframes and "lollipops" obtained using MorphoJ (version 1.06d, Klingenberg, 2011, 2013). PCA plots for fitted values were also produced in R (version 4.1.1). Fitted values are models prediction of mean response values when factor levels have been inputted, in our case, molar type and stratigraphic unit. Thin-plate splines were used to aid visualisation of deformation along principal component vectors.

A test of allometry (analysis of variance using residual randomisation) was carried out in R (version 4.1.1; Geomorph, version 4.0; RRPP, version 1.0; R Core Team, 2021) using natural log transformed centroid size and Procrustes coordinates in order to assess the power

of allometric signal in the total sample of molar shapes and whether it changes between molar types. Subsequently, allometry was tested within each individual molar separately and visualised with consensus thin-plate spline deformation grids for each stratigraphic unit within each tooth type produced in TPSSplin (version 1.25; Rohlf, 2004).

Finally, Phenotypic trajectory analysis (PTA) was used to test whether individual molar shape changes occur in a similar way throughout the same temporal sequence. Phenotypic evolutionary trajectories are a sequence of ordered estimated phenotypes along a given path, in this case, one path (defined by units) for each tooth type (M_1, M_2 and M_3). The vectors in each evolutionary path are connected by the mean shape (within each tooth type) from the oldest (4A) to the youngest (1A) chronostratigraphic unit. Each vector is characterised by three components: size ($MD_{1,2}$), direction ($\theta_{1,2}$), and shape (D_{Shape}). The analysis of these three attributes provides a complementary methodology in testing temporal phenotypic evolution.

Trajectory size is the vector length distance along an evolutionary path or trajectory and is defined as the sum of the distances between evolutionary levels (Adams and Collyer, 2009). Differences in shape trajectories can be used to understand acceleration or deceleration of shape change through time and are represented by Euclidean distances across levels between scaled and aligned phenotypic trajectories. Trajectory direction or orientation is described by the direction of its first principal component of its covariance matrix. For each trajectory, a PCA is performed. Pairwise angular differences are then obtained between the first principal components of different trajectories providing an angle statistic in degrees of one vector to another (Adams and Collyer, 2009). Trajectory shape corresponds to evolutionary levels expressed in data space, found from the deviations between corresponding evolutionary levels across two scaled and aligned phenotypic trajectories. This is only supplied when analysing phenotypic trajectories of three or more levels (three levels

in each tooth type in our case) and is expressed as Euclidean distance (D_{Shape}). Trajectory vectors with only two levels lack the shape attribute, only possessing size and direction. A description of the shape of a configuration of points is accomplished using Procrustes analyses. Differences in trajectory shapes imply that there is a signal, that at a unique time, specific shape change is occurring (Adams and Collyer, 2009).

In regard to our dataset, differences in trajectory shape through evolutionary levels (chronostratigraphic units), infer that changes in one or multiple portions of the trajectories in shape are accelerated or decelerated by one unit relative to another within tooth types, or that they are orientated in different directions, or both accelerated/decelerated and orientated in different directions (Collyer and Adams, 2013). This is expressed as Euclidian distance or D_{Shape}. Trajectory shape differences use a least-squares superimposition alignment and are found from deviations between examined levels of aligned phenotypic trajectories. For all attribute differences, $MD_{1,2}$, $\theta_{1,2}$ and D_{Shape}, after 1000 permutations were considered significant when P values were below an acceptable error rate $\alpha = 0.05$. $MD_{1,2}$, and D_{Shape} statistics originate from PCA scores that are unitless, while $\theta_{1,2}$ is given in degrees (°). The evolutionary vectors represented temporal shape changes that covered ca. 90,000 years from MIS 5 to MIS 3 across M_1, M_2 and M_3. These were compared using R (version 4.1.1; Geomorph, version 4.0; RRPP, version 1.0; Adams and Collyer, 2009; Adams and Otarola-Castillo, 2013; R Core Team, 2021).

3. Results

3.1. Tooth Size

ANOVA revealed differences in size (LnCS) between tooth types ($F_{2,515} = 289.953$, $r^2 = 0.50$, $P < 0.001$) and stratigraphic units (ANOVA, $F_{2,515} = 17.49$, $r^2 = 0.034$, $P < 0.001$) with a pattern of $M_1 < M_2 < M_3$ (Fig. 4) occurring for each stratigraphic unit (Table 6).

When analysed separately, there was no evidence of M_1 size difference between stratigraphic units (ANOVA, $F_{2,188} = 0.7418$, $r^2 = 0.0078$, $P < 0.491$; Fig. 4, Table 3 and Table S2). M_2 showed significant temporal variation in size (ANOVA, $F_{2,230} = 18.802$, $r^2 = 0.14$, $P < 0.001$). Pairwise tests show M_2 teeth from unit 1A to be significantly larger than all the other layers (Fig. 4, Table 3). Allometric shape changes in M_2 (Table S4) differ between stratigraphic units.

ANOVA detected temporal changes in M_3 (ANOVA, $F_{2,97} = 6..2578$, $r^2 = 0.114$, $P < 0.007$). Pairwise comparisons of M_3 size showed differences between unit 1A (larger teeth) when compared to unit 3 and 4A ($P < 0.01$), while no other pairwise tests were significant (Table 3).

Tooth Type	Units	d	UCL	Z	$>P$
M_1	1A:3	0.005975	0.019827	-0.157523	0.564
	1A:4A	0.007872	0.020496	0.074977	0.492
	3:4A	0.01384?9	0.022114	0.816422	0.22
M_2	1A:3	0.0488337	0.020691	3.398704	**0.001**
	1A:4A	0.0560678	0.023556	3.468273	**0.001**
	3:4A	0.0072341	0.024436	-0.106469	0.559
M_3	1A:3	0.06253736	0.0414181	2.4183426	**0.003**
	1A:4A	0.05245558	0.04019562	2.0901576	**0.014**
	3:4A	0.01008178	0.0424373	-0.3215703	0.618

Table 3. Pairwise comparisons for M_1, M_2 and M_3 expressed with P values using natural logarithm of centroid size (significance indicated in **bold**) for each stratigraphic unit within each tooth type.
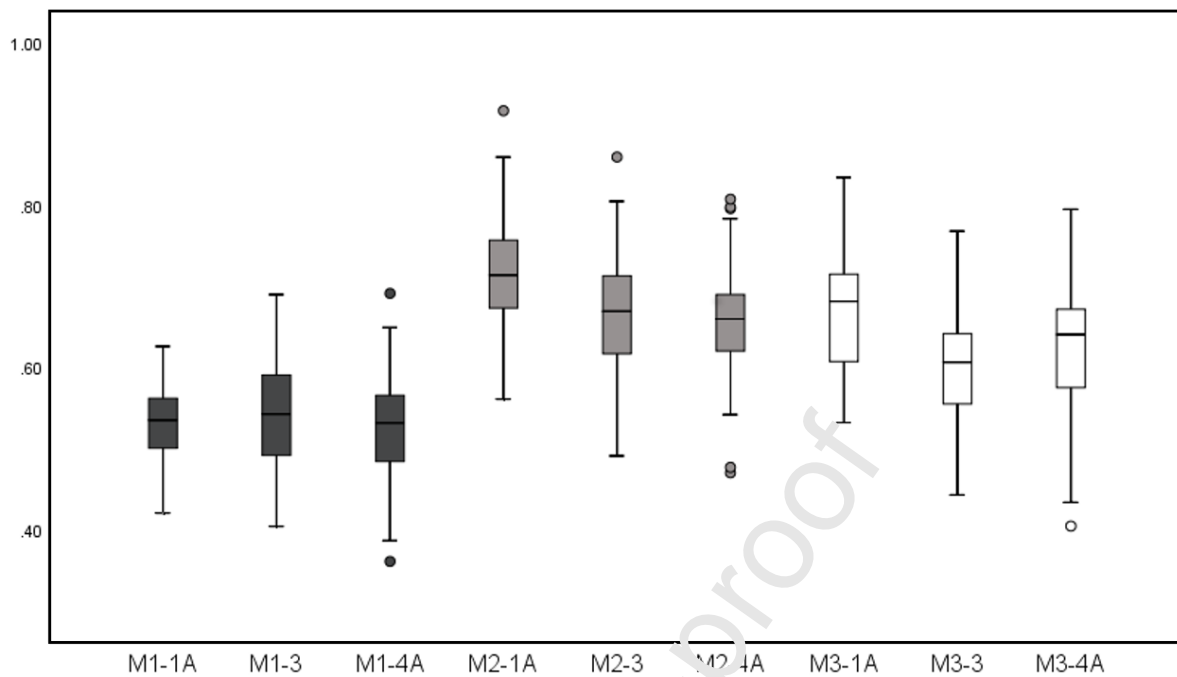
Figure 4. M_1, M_2 and M_3 box blots showing differences in natural logarithm of centroid size. Data for M_1 are presented in dark grey, M_2 in light grey and M_3 in white boxes.

3.2.Tooth shape variation and Phenotypic Trajectory Analysis

Procrustes ANOVA of shape data showed statistically significant differences between tooth type and stratigraphic unit (Table 4). Overall, tooth type explained 57.15% of variation and unit explained only 0.65%. PCA scatter plots help visualize shape difference in tooth type detected by Procrustes ANOVA (Figure 5), with PC1 (63.46%) explaining a substantial proportion of shape variation in the total sample while large overlap occurred across stratigraphic units (Figure 5a). Negative PC1 scores describe M_1 dentition with an elongated occlusal surface shape relative to an expanded mesial entoconid to distal entoconid distance and contraction between the protoconid and metaconid. Further progression along the tooth row presents a buccolingual relative expansion in M_2 described by neutral scores and a

further widening in M_3 relative to an expansion between buccal and lingual cusps described by positive PC1 scores. This is conveyed through expansion between the protoconid and metaconid at the mesial end of the occlusal surface and a contraction between the mesial and distal entoconids at the distal end of the tooth. PC2 (12.25%) shows a strong mesiodistal contraction, related to the positioning of the mesial entoconid and an expansion and contraction between the distal entoconid and hypoconid (negative and positive PC2, respectively). PC2 shows a general neutral positioning of M_1 and M_2 dentition (position scores between +0.1 to -0.1), while M_3 varies more in this aspect of shape across the sample. PCA on individual tooth types separated by stratigraphic unit are presented within the supplementary material (Figure S1, S2 and S3).

There is a significant allometric signal on tooth shape ($F_{1, 523} = 163.6726$, $r^2 = 0.12737$, $P < 0.007$) and allometric trajectories change between tooth types ($F_{2, 518} = 7.6495$, $r^2 = 0.01191$, $P < 0.007$) (Table 4). When analysed separately, M_2 and M_3 shape variation was significantly impacted by size (M_2: $r^2 = 0.0115$, $P = 0.033$; M_3: $r^2 = 0.08$, $P < 0.007$; Figure 6), while no allometric effect could be detected on the shape of M_1 specimens ($P > 0.05$; Table S2). Allometric shape changes in both M_2 and M_3 differ between stratigraphic units (M_2: $F = 2.6886$, $df_{1, 231}$, $r^2 = 0.0115$, $P < 0.033$; M_3: $F = 8.6293$, $df_{1, 98}$, $r^2 = 0.08093$, $P < 0.007$). Within M_2 specimens, only unit 1A specimens showed significant allometry ($r^2 = 0.058031$, $P < 0.0001$). M_3 specimens exhibited high levels of allometry, with significant results in all groups (1A: $r^2 = 0.119$, $P < 0.003$; 3: $r^2 = 0.1057$, $P < 0.03$; 4: $r^2 = 0.0831$, $P < 0.03$) (Table S4).

Average tooth shape by tooth type were plotted to show vector differences along PC1 and PC2 for fitted values (Figure 5b; Table 5) which are the models prediction of mean response values when factor levels have been inputted. Directions of shape change were largely consistent in M_1 and M_2, however significant differences in $MD_{1, 3}$ and $MD_{2, 3}$ were

found for M_3 comparisons ($P < 0.002$, Table 5). M_3 exhibited significantly more shape change than M_1 ($d = 0.0796$, $P < 0.001$) and M_2 ($d = 0.0626$, $P = 0.002$) based on vector size corresponding to an accelerated shape change through time for M_3. Analyses of principal vector angles ($\theta_{1, 2}$) showed that evolutionary trajectory direction changes through time are similar between M_1 and the other two lower molars considering that the observed angles were significantly smaller than the upper confidence limit computed under random expectation (Table 5). The only significant difference in directional shape change was between M_2 and M_3 with an angle significantly larger than random expectation ($\theta = 127.03°$, Table 5). Trajectories did not differ in shape between any tooth types (D_{shape}, Table 5). This corresponds to neither a decrease or acceleration in shape change between tooth types.

Plotting the averaged tooth shape change by layer allows to visual assessment of the unique pattern of variation observed in M_3 (Fig. 6). Deformation grids in M_1 do not significantly stretch between layers with landmark configuration maintaining a configuration pretty similar to average shape while in M_2 the average shape of layer 3 appears significantly different from that of the other layers due to the change in the relative position of the mesial metaconid and mesial entoconid. These landmarks vary even more in M_3 with a progressive expansion through stratigraphic units (Fig. 6c). Such variation corresponds to the wider portion of morphospace occupied by M_3 in PCA plots (Fig. 5).

	F	Z	df	r^2	$P <$
Size tooth type	289.95	12.913	2, 515	0.5042	**0.001**
Size unit	17.491	4.6404	2, 515	0.0342	**0.001**
size tooth type x unit	5.0377	3.2098	4, 515	0.0175	**0.001**
Shape tooth type	366.87	9.5548	2, 515	0.5715	**0.001**
Shape unit	4.1482	3.2503	2, 515	0.0646	**0.001**
Shape tooth type x unit	6.7037	5.9287	4, 515	0.0209	**0.001**

Allometry of tooth shape	163.67	7.4996	1, 523	0.1274	**0.007**
Allometric change between tooth type	7.6495	5.5505	2, 518	0.0119	**0.007**

Table 4. ANOVA for size and shape of tooth type, unit, tooth type/unit interaction and allometry of tooth shape and between tooth types containing r^2 and P values (significance indicated in **bold**).

$MD_{1,2}$	Unit	d	UCL	Z	P
	M_1:M_2	0.0169	0.0259	0.9549	0.174
	M_1:M_3	0.0796	0.0327	3.4215	**0.001**
	M_2:M_3	0.0626	0.0352	2.7683	**0.002**
$\theta_{1,2}$	Unit	Angle (°)	UCL	Z	P
	M_1:M_2	44.259	130.0721	-0.4662	0.652
	M_1:M_3	123.42	131.1191	1.5504	0.072
	M_2:M_3	127.03	125.9122	1.6419	**0.045**
D_{Shape}	Unit	d	UCL	Z	P
	M_1:M_2	0.0959	0.5842	1.4543	0.918
	M_1:M_3	0.1038	0.6239	-1.4963	0.922
	M_2:M_3	0.0945	0.6388	-1.5652	0.937

Table 5. Summary statistics for differences in phenotypic trajectory size ($MD_{1,2}$), direction ($\theta_{1,2}$), and shape (D_{Shape}) between M_1, M_2 and M_3. Scores for d (trajectory length), upper confidence limits (UCL) Z, P and angle (°) have been provided (significance indicated in **bold**).
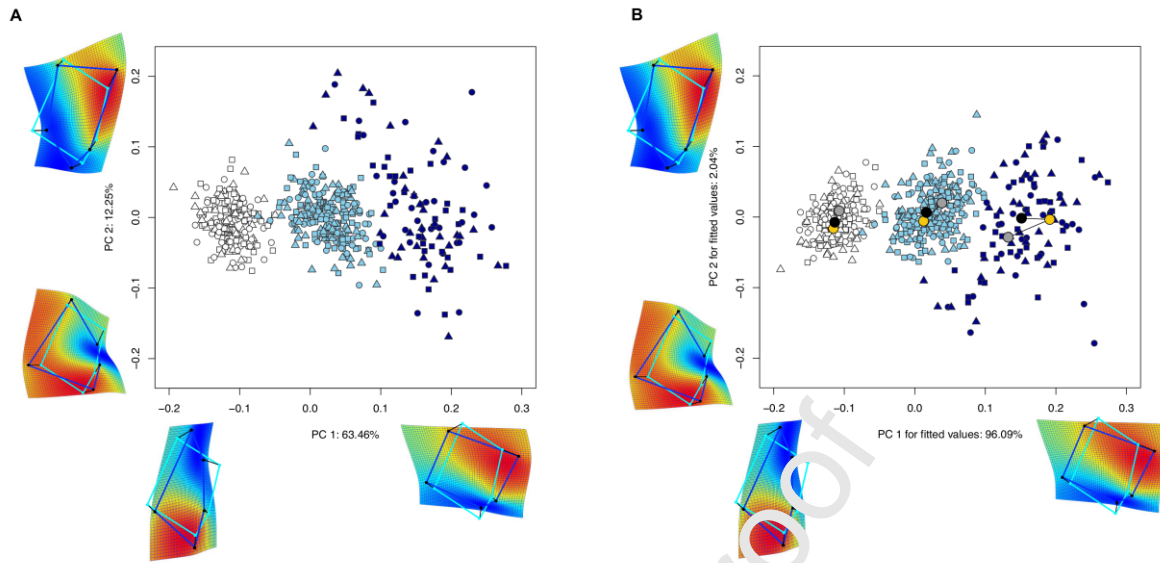
Figure 5. (**A**) PC plot of original shape coordinates PC1 (63.46%) and PC2 (12.25%) for M_1, M_2 and M_3. (**B**) PC plot of PC1 (96.09%) and PC2 (2.04%) for M_1, M_2 and M_3 with evolutionary trajectory means for fitted values. For both **A** and **B**, M_1, M_2 and M_3 are represented by white, sky blue and dark blue points, respectively. Units 1A, 3 and 4A are represent by circles, squares and triangles, respectively. Large circles represent average phenotype for each group (stratigraphic unit: 1A - grey, 3 - yellow, 4A -black). Temperature related Jacobean expansion factors have been used as a visual aid on deformation grids (blue shows contraction, red shows expansion) accompanied by two coloured wireframes to show mean shape (light blue) and deformation (dark blue) at the extremity of the principal component.
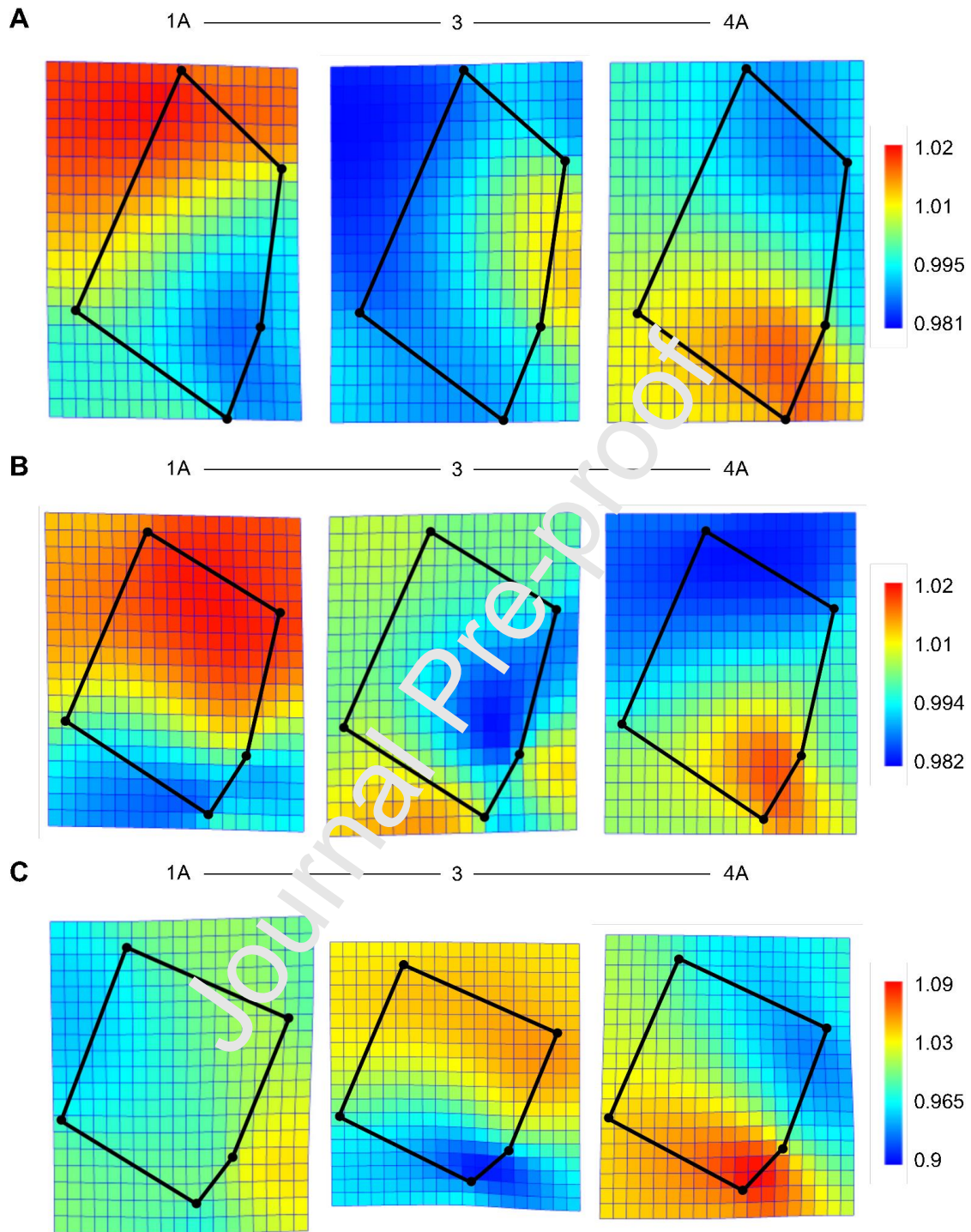
Figure 6. Tooth shape variation associated with size showing consensus deformation of each stratigraphic unit within each tooth type from the group mean. (**A**) deformation grids of stratigraphic units 1A (LnCS = 0.53), 3 (LnCS = 0.54) and 4A (LnCS = 0.52) (*left to right*) of

M$_1$. (**B**) deformation grids of stratigraphic units 1A (LnCS = 0.72), 3 (LnCS = 0.67) and 4A (LnCS = 0.66) (*left to right*) of M$_2$. (**C**) deformation grids of stratigraphic units 1A (LnCS = 0.67), 3 (LnCS = 0.60) and 4A (LnCS = 0.61) (*left to right*) of M$_3$. Temperature related Jacobean expansion factors have been used as a visual aid on deformation grids, blue shows contraction, red shows expansion.

	M$_1$	M$_2$	M$_3$
1A	0.531	0.715	0.725
3	0.537	0.666	0.757
4A	0.523	0.660	0.773

Table 6. Mean LnCS for each stratigraphic unit within each tooth type.

4. Discussion

Molariform dentition of cave bears have demonstrated progressive modification, with the rate of change in the occlusal surface suggested to increase during the late Pleistocene (Rabeder and Tsoukala, 1990). Many studies have underpinned the hypothesis that environmental changes stimulated phenotypic adaptations in fossil bears (Baryshnikov *et al*., 2003, 2004; Rabeder *et al*., 2011; Robu *et al*., 2013, 2018; Bocherens *et al*., 2014b). In this study, we show an increase in lower molar tooth size from MIS 5 – MIS 3, with a temporal variation in cusp position, relating to a larger talonid grinding platform in later, more climatically harsh time periods. Changes relating to a morphologically larger talonid section in lower cheek teeth are found in M$_2$ and M$_3$, with M$_3$ showing a more morphologically divergent change suggesting that this tooth is much more responsive to habitat changes than the molars before it. Tooth type further follows a constant pattern of relative tooth size

variation, *i.e.*, $M_1 < M_2 > M_3$ across all time periods. This developmental pattern has been previously identified in the family Ursidae (Asahara *et al*., 2016).

The inhibitory cascade model (IC, Kavanagh *et al*., 2007; Renvoisé *et al*., 2009; Jernvall and Thesleff, 2012) proposes that the size of lower molars in mammals are controlled by molecules produced by the M_1 tooth germ and certain taxa follow particular regression lines in M_1/M_2 vs M_3/M_1 morphospace. This model has been used to explain variation in lower molars and the loss of third molars in mammals. The model states that molar tooth row sizes vary from $M_1 > M_2 > M_3$ to $M_1 = M_2 = M_3$ to $M_1 < M_2 < M_3$ and can explain variation throughout mammalian species, with ursids being one of the few exceptions (see Kavanagh *et al*., 2007 for details on statistics). The model statistics have been recently simplified in a study by Roseman and Delezene (2019), where IC predictions for M_3 tooth size can be calculated by $M_3 = 2*M_2 - M_1$. Asahara and colleagues (2016) suggested that ursids exhibit a $M_1 < M_2 > M_3$ pattern that cannot be explained by the inhibitory cascade model. Findings herein support this concept. However, recent studies contradict the model (Roseman and Delezene 2019; Baryshnikov and Puzachenko, 2020). Baryshnikov and Puzachenko (2020) found results for ursids and *U. spelaeus* specifically in relation to the IC model. They only detected a relationship in the tooth row when P_4 dentition was included in the model and presented the lower molar tooth row pattern: $M_1 \approx M_2 > M_3$ (which was also largely linear). The IC model uses relative molar length when understanding patterns in mammalian tooth rows. However, when using LnCS in regard to the IC model, our results show a $M_1 < M_2 < M_3$ across all stratigraphic units studied. This pattern conforms to the IC model and may suggest that GMM is a more accurate methodological tool when describing the size of complex shapes.

The increase in lower molar tooth size through time concords with findings relative to the upper molariform dentition of specimens from the same chronostratigraphic sedimentary

deposits of Scladina (Charters *et al*., 2019). An increase in M^2 size from unit 4A – 1A (MIS 5 to MIS 3) correlates with an increase in M_2 and M_3 size throughout the sedimentary units. This increase in molar size is shown in M_1, M_2 and M_3 dentition studied herein and the direction of change is temporally sequential throughout all dentition for both length and width measurements (Table S3).

M^2, M_2 and M_3 occlude during mastication to create a large grinding platform for the consumption of foliage and mast. This analogous morphological change would aid in maintaining biomechanical performance for adept mastication. Recent biochemical and biomechanical studies have proposed that cave bears had adapted a diet exclusive to foliage and mast from ~100ka (Bocherens, 2019) and were further dietary restricted to consuming low energetic plant material during pre-dormancy (Pérez Ramos *et al*., 2020).

Available food sources in environments can be studied through palynological analyses of sedimentary deposits, giving insight into plant species and their abundance in an environment at a specific temporal interval. Palynology relating to units 4A, 3 and 1A (MIS 5-3) suggest a gradual environmental shift from a temperate to boreal to a more steppic environment (Pirson *et al.,* 2008; 2014), inferred by the representation and abundance of plant species in the related sedimentary infill. Unit 4A (relating to MIS 5 with later chronostratigraphic layers in the unit possibly in early MIS 4) is composed of a multitude of layers pertaining to different geological processes. Palynological analysis of the unit, suggests temperate conditions with relatively high percentages of various temperate malacophyll trees, high levels of algae and the presence of a thick stalagmitic floor indicating climatic improvements in the palaeoenvironment (Bastin *et al*., 1986; Gullentops and Deblaere, 1992; Quinif *et al.,* 1994; Pirson *et al.,* 2008; 2014). Unit 3 is suggested to have a lower tree rate than that in 4A, but still strongly represented by deciduous and coniferous trees, followed by the later environment (unit 1A) dominated by herbs, grasses and flowering

plants. Further pollen, insect and plant macrofossil studies of European palaeoenvironments during MIS 5 to MIS 3 suggest a transition from the peak of an interglacial (Eemian interglacial), generally characterised by long intervals of temperate forests across mainland Europe (Jung *et al*., 1972; Helmens, 2014), encompassing vast tundra landscapes with inadequate comestible plant material for herbivorous megafauna like the cave bear to thrive on. Taken together, these findings suggest that climatic cooling, lack of dietary flexibility and related food source availability during pre-dormancy may have played a pivotal role in the morphological adaptation of molariform dentition and the later extinction of the species (Baca *et al*., 2016). The palynology of the studied stratigraphic chronology further supports this morphological adaptation of an increased molar size and a coordinated evolutionary expansion of the talon/talonid in cave bear molars.

Research on habitat tracking may offer a different view on the results herein. Raia and colleagues (2012) suggest that mammalian species respond to environmental change by dispersing to new environments with better ecological conditions as opposed to those affected by climatic decline, actively tracking similar ecological conditions in a new area. This in turn would keep morphology stable and different morphologies and genetic lineages may represent morphological change through time. Due to the strong link between habitat and dental morphology of mammals, habitat tracking from one environment to another of similar ecological position would suggest a stasis of morphological change. However, research into habitat tracking of fossil species is limited and the reliability of results when reproducing distances tracked of an extinct species while in existence may be questionable.
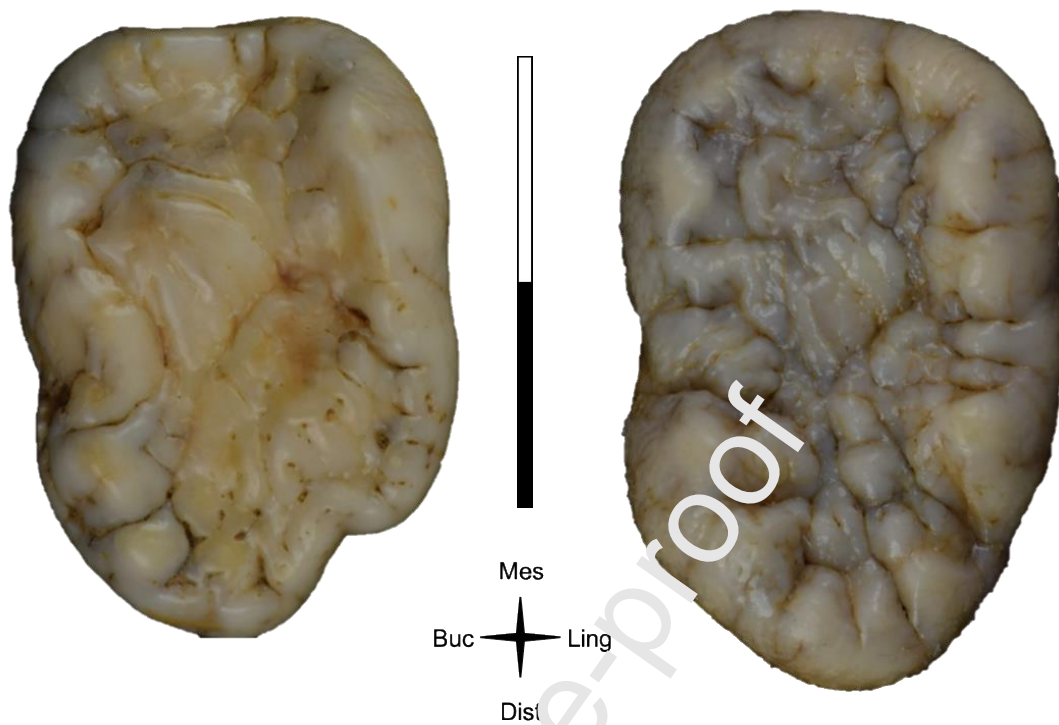
Figure 7. M$_3$ dentition of *U. spelaeus* from unit 1A showing varying shape deformation at mesial/distal entoconid (*left*: SC-86-132-1-625, *right*: SC-89-120-619).

Trophic diversity due to environmental differences have been found to impact functional mandibular morphology in extant bears (Meloro *et al*., 2017). This is further corroborated by studies based on bear tooth microwear (Pappa *et al*., 2019), while tooth dimensions have been previously used to separate bear dietary groups (Van Valkenburgh, 1988; Sacco & Van Valkenburgh 2004). Smaller molariform dentition have been found to relate to more carnivorous ursids, being progressively larger in omnivores and more so in herbivorous species (insectivores have little need for further processing of food) (Sacco and Van Valkenburgh, 2004). In this respect, differences in M$_2$ and M$_3$ tooth morphology have

been suggested as adaptive when bears occupy different ecological niches (Baryshnikov *et al.*, 2003). PCA further show functional morphological changes in the occlusal surface of the dentition studied from temporally distinct environments (Figure 5). PC1 shows the majority of variation in the sample and visually describes the variation between tooth types. Size has a significant effect on shape in the occlusal position of cusps, further clarified by a strong allometric signal and supported by r^2 values (Table 4). Specimens of M_3 exhibited significant levels of allometric effect in comparison to M_1 and M_2 dentition (Table 4 and S2).

Although analyses of specimens in units within each tooth type did not suggest strong visual patterns (PCA, Figure 5, S1, S2 and S3), statistical analysis revealed significant change between units occurs in all tooth types (Table 4). In M_1, deformations in units 3 and 4A show differences in mean shape with a relative lengthening both mesially and distally on the lingual side between the metaconid and the distal entoconid, with the opposite shown in unit 1A specimens. However, 1A specimens show a buccolingual expansion in tooth shape, seemingly in conjunction with the buccolingual expansion of both M_2 and M_3 specimens. Mean shape change is also shown in specimens of M_2, with similar cusp positioning shown in 1A specimens (Fig. 6). A buccolingually contracted tooth shape in unit 3 and 4A dentition manifests the lesser need for a large talonid section in these environments (MIS 4-5). M_3 shape data shows a more mesial positioning of the protoconid and metaconid along with a distally increased position of the distal entoconid, more so in unit 1A specimens. This, in turn, would maintain biomechanical performance with the correlated expansion between the post-hypocone and hypocone (resulting in a larger talon section) shown in M^2 specimens from the same stratigraphic sedimentary units (Charters *et al.*, 2019). M_3 specimens further show contraction between mesial and distal positioned cusps, accompanied by a contraction between the mesial and distal entoconid. This relates to some specimens forming a crease between the two cusps, deforming the outer shape of the tooth (Figure 7). This linguo-distal

indent varies greatly, even between specimens from the same evolutionary time-period. Factors such as tooth row constraint or mandibular morphology may shed light into this morphological variant.

Baryshnikov and Puzachenko (2020) suggested that the cave bear *U. kudarensis* (a large cave bear species found in the Caucasus and Eastern Siberia region) showed specific evolutionary modifications in molariform dentition and even detected individual modifications in specimens of M_3. In cave bears, the morphology of the mandibular corpus and ramus creates space distally of the M_3, expressing a lingually elongated corpus, allowing room for more varied adaptation in molariform dentition, especially for a well-developed grinding platform to be housed (Van Heteren *et al*., 2009, 2014, 2016; Meloro, 2011). In other herbivores such as *A. melanoleuca* (Giant Panda), the morphology of the mandibular corpus and ramus limits the space for distal expansion of the third lower molar. Expansion of M_3 occurs lingually behind the ramus (Sacco and Van Valkenburgh, 2004) possessing a shorter mandibular corpus at the molars relative to the premolars, with the tooth row ending at the corpus/ramus threshold (Meloro, 2011, Meloro *et al*., 2017). This relates to the previously mentioned IC model and may explain the non-conformity in ursids (Asahara *et al*., 2016).

Phenotypic trajectories show non-independent paths of evolutionary changes in M_1 and M_2 dentition. However, vector sizes are statistically different in M_3 means compared to those of M_1 and M_2. This shows that phenotypic changes in tooth types between units in M_1 and M_2 produce similar vector lengths (Table 5). Again in $\theta_{2, 3}$, M_3 shows evolutionary vector angles that differ from M_2. It should be noted that comparisons in vector angles between M_1 and M_3 dentition are non-significant ($\theta_{1, 3} = 123.42°$, UCL = 131.12, P = 0.072), however, *P* values and vector angles are very similar to that between M_2 and M_3 that show a trajectory angle significantly larger than random expectation ($\theta = 127.03°$, Table 5). This suggests

evolutionary parallelism in trajectories of M_1 and M_2 dentition based on trajectory size, direction and shape, while M_3 follows a different path. D_{Shape} further supports evolutionary parallelism between dentition. Phenotypic means of M_1 and M_2 suggest change to a wider shape through time, whereas M_3 shows scattered specimens across the morphospace but a movement of general phenotypic shape to an expanded talonid section in unit 1A specimens in relation to a wider/shorter cusp position in unit 3 specimens previous. Phenotypic trajectory means suggest an adaptation to create a larger grinding platform to consume more fibrous plant material due to climatic and environmental pressures of MIS 3 (Baryshnikov *et al.*, 2003; Daura *et al.*, 2017). Phenotypic trajectories changes show similarity between M_1 and M_2, suggesting parallel evolution (Stayton, 2006; Adams and Collyer, 2009). This supports coordinated shape changes in molariform dentition that is more impacted by spatial constraint within the mandibular corpus.

On the other hand, the divergent variation of M_3 suggests that this tooth is less constrained (developmentally) to expand or shrink, so it appears much more responsive to environmental changes. This further corroborates the hypothesis that cave bears from Scladina expanded their herbivorous feeding niche during the latest glacial in response to food availability. Perhaps such a level of dietary specialisation might have also been the reason of its further extinction. With the argument of the cave bear diet becoming more evident in regard to it being a hyper-specialized herbivore (minus small populations of debate; Richards *et al.*, 2008; Robu *et al.*, 2013, 2018; Bocherens, 2019), answers regarding extinction and diet have become more solid.

Through population demographics, Mondanaro and colleagues (2019) suggested that climatic and environmental factors were responsible for a 10-fold decrease in cave bear populations after ca. 40ka, but this could not fully explain the extinction of the species.

Dating of recent assemblages do, however, corroborate an extinction by climatic decline. Radiocarbon dating has provided an extinction date of 26.1 – 24.3 Ka, this falls within the Greenland Stadial 3, the coldest period of the last glacial (Peltier and Fairbanks, 2006; Clark *et al*., 2009; Cooper *et al*., 2015). This climatic decline suggests reduced vegetation due to climatic deterioration was key to the demise of the cave bear (Barnosky *et al*., 2004; Koch and Barnosky, 2006; Lorenzen *et al*., 2011; Cooper *et al*., 2015; Stuart, 2015; Baca *et al*., 2016), supported by findings herein.

5. Conclusion

Phenotypic trajectory analysis confirms suggestions from size and shape analyses through GMM of a temporal size increase and cusp movement to house a larger talonid platform to process more fibrous plant material relating to climatic decline. The divergent variation of M_3 suggests that this tooth is less constrained and appears much more responsive to environmental changes. This is shown over short temporal intervals from MIS 5 to MIS 3. Further, findings also corroborate with those found in the upper molars from specimens of the same stratigraphic deposits and that of recent $\delta^{15}N$ stable isotopic analyses suggesting complete herbivory of *U. spelaeus* in the latter one-hundred-thousand-years of the species existence. The pernicious effect of this extreme dietary inflexibility and hyper-specialization, evidently, would be a critical factor in the demise of the species.

Conflict of interest

There are no conflicts of interest.

Funding sources

Acknowledgements

We would like to thank the team at Scladina Cave Archaeological Centre for their hard work and granting access to the specimens used in this study. We would further like to thank the three anonymous reviewers who's comments helped greatly to improve this manuscript.

References

Abrams, G., Bello, S. M., Di Modica, K., Pirson, S., Bonjean, D. 2014. When Neanderthals used cave bear (Ursus spelaeus) remains: Bone retouchers from unit 5 of Scladina Cave (Belgium). Quaternary International. 326- 327:274–287.

Abrams, G., Bonjean, D., Di Modica, K., Pirson, S., Otte, M., Patou-Mathis, M. 2010. Les os brulés de l'ensemble sedimentaire 1A de Scladina (Andenne, Belgique): apports naturels ou restes se foyer(s) néandertalien(s)?. In: Notae Praehistoricae. 30, 5-13.

Adams D.C., Collyer M.L. 2009. A general framework for the analysis of phenotypic trajectories in evolutionary studies. Evolution 63: 1143–1154.

Adams, D.C., Collyer, M.L. 2015. Permutation tests for phylogenetic comparative analyses of high-dimensional shape data: what you shuffle matters. Evolution 69, 823-829.

Adams, D.C., Otárola-Castillo, E. 2013. Geomorph: an R package for the collection and analysis of geometric morphometric shape data. Methods in Ecology and Evolution. 4, 393-399.

Adams, D. C., Collyer, M. L., Kaliontzopoulou, A., Balken. E. K. 2021. Geomorph: Software for geometric morphometric analyses. R package version 4.0. https://cran.r-project.org/package=geomorph.

Adams, D.C., Rohlf, F.J., Slice, D.E. 2004. Geometric morphometrics: ten years of progress following the 'revolution'. Italian Journal of Zoology. 71, 5-16.

Adams, D.C., Rohlf, F.J., Slice, D.E. 2013. A field comes of age: geometric Morphometrics in the 21st century. Hystrix, the Italian Journal of Mammalogy. 24, 7-14.

Asahara, M., Saito, K., Kishida, T., Takahashi, K., Bessho, K., 2016. Unique pattern of dietary adaptation in the dentition of Carnivora: its advantage and developmental origin. Proceedings of the Royal Society B: Biological Sciences, 283(1832), p.20160375.

Ashton, K. G., Tracy, M. C., de Queiroz, A. 2000. Is Bergmann's rule valid for mammals? American Naturalist 156:390 – 415.

Athen, K., Frömke, C., Germonpré, M. 2005. Analysis of postcranial elements of cave bear material (*Ursus spelaeus*) from Goyet (Condroz/Belgium). Bulletin de l'Institut royal des sciences naturelles de Belgique, Série Sciences de la terre 75, 267–283.

Baca, M., Popović, D., Stefaniak, K., Marciszak, A., Urbanowski, M., Nadachowski, A., Mackiewicz, P. 2016. Retreat and extinction of the Late Pleistocene cave bear (*Ursus spelaeus sensu lato*). The Science of Nature. 103, 92.

Baken, E. K., M. L. Collyer, A. Kaliontzopoulou, and D. C. Adams. 2021. gmShiny and geomorph v4.0: new graphical interface and enhanced analytics for a comprehensive morphometric experience. Methods in Ecology and Evolution. Submitted.

Barnosky, A. D, Koch, P. L, Feranec, R. S, Wing, S. L, Shabel, A. B. 2004. Assessing the causes of late Pleistocene extinctions on the continents. Science. 306:70–75.

Baryshnikov, G. 2007: Bears Family (Carnivora, Ursidae). Nauka, St. Petersburg (Fauna of Russia and Neighboring Countries, new series 147) (in Russian). 541.

Baryshnikov, G., Foronova, I. 2001. Pleistocene small cave bear (Ursus rossicus) from the South Siberia, Russia."Cadernos Lab. Xeolóxico de Laxe Coruña. 2001. Vol. 26, pp. 373-398

Baryshnikov, G. F., Puzachenko, A. Y. 2011. Craniometrical variability in the cave bears (Carnivora, Ursidae): multivariate comparative analysis. Quaternary International. 245, 350-368.

Baryshnikov, G. F., Puzachenko, A. Y. 2018. Morphometry of upper cheek teeth of cave bears (Carnivora, Ursidae). Boreas. 12360.

Baryshnikov, G. F., Puzachenko, A. Y. 2020. Morphometry of lower cheek teeth of cave bears (Carnivora, Ursidae) and general remarks on the dentition variability. Boreas, Vol. 49, pp. 562–593

Baryshnikov, G., Germonpré, M., Sablin, M. 2003: Sexual dimorphism and morphometric variability of cheek teeth of the cave bear (*Ursus spelaeus*). Belgian Journal of Zoology 133, 111–119.

Baryshnikov, G., Mano, T., Masuda, R. 2004. Taxonomic differentiation of *Ursus arctos* (Carnivora, Ursidae) from south Okhotsk Sea islands on the basis of morphometrical analysis of skull and teeth. Russian Journal of Theriology 3, 77–88.

Bastin B., Cordy J.-M., Gewelt M., Otte M. 1986. Fluctuations climatiques enregistrées depuis 125.000 ans dans les couches de remplissage de la grotte Scladina (province de Namur, Belgique). Bulletin de l'Association française pour l'Étude du Quaternaire, 2e série, 25-26: 168–177.

Bastir, M., Higuero, A., Rios, L. and Garcia Martinez, D. 2014. Three-dimensional analysis of sexual dimorphism in human thoracic vertebrae: Implications for the respiratory system and spine morphology. American Journal of Physical Anthropology, 155(4), pp.513-521.

Bergmann, C. 1847. Über die Verhältnisse der Wärmeökonomie der Thiere zu ihrer Grösse. Göttinger Studien 3:595–708.

Bocherens, H. 2015. Isotopic tracking of large carnivore palaeoecology in the mammoth steppe. Quaternary Science Reviews. 117:42–71.

Bocherens, H. 2019. Isotopic insights on cave bear palaeodiet. Historical Biology 31, 4, 410-421

Bocherens, H., Billiou, D., Patou-mathis, M., Bonjean, D., Otte, M., Mariotti, A., 1997. Paleobiological implications of the isotopic signatures (13C, 15N) of fossil mammal collagen in Scladina Cave (Sclayn, Belgium). Quaternary Research. 48, 370-380.

Bocherens, H., Billiou, D., Patou-mathis, M., Otte, M., Bonjean, D., Toussaint, M., Mariotti, A. 1999. Palaeoenvironmental and palaeodietary implications of isotopic biogeochemistry of

late interglacial Neandertal and mammal bones in Scladina Cave (Belgium). Journal of Archaeological Science. 26(6), pp.599–607.

Bocherens, H., Drucker, D.G., Billiou, D., Geneste, J.M., van der Plicht, J., 2006. Bears and humans in Chauvet Cave (Vallon-Pont-d'Arc, Ardeche, France): insights from stable isotopes and radiocarbon dating of bone collagen. Journal of Human Evolution. 50, 370-376.

Bocherens, H., Baryshnikov, G., van Neer, W. 2014a. Were bears or lions involved in salmon accumulation in the Middle Palaeolithic of the Caucasus? An isotopic investigation in Kudaro 3. Quaternary International. 339– 340:112–118.

Bocherens, H., Bridault, A., Drucker, D. G., Hofreiter, M., Münzel, S. C., Stiller, M., van der Plicht, J. 2014b: The last of its kind? Radiocarbon, ancient DNA and stable isotope evidence from a late cave bear (*Ursus spelaeus* Rosenmüller, 1794) from Rochedane (France). Quaternary International 339–340, 179–188.

Bonjean, D. 1995. Dans la foulée de l'Homme de Neandertal: Sclayn 1994. In: Plumier J, Corbiau M-H, editors. Troisième journée d'Archeologie Namuroise, Namur. Ministère de la Région wallonne, DGATLP, Direction de Namur, Service des fouilles. p. 45–48.

Bonjean, D., Di Modica, K., Abrams, G., Pirson, S., Otte, M., 2011. La grotte Scladina: bilan 1971-2011. In: Toussaint, M., Di Modica, K., Pirson, S. (Eds.), Le Paléolithic moyen en Belgique. Mélanges Marguerite Ulrix-Closset. Bulletin de la Société Royale Belge d'Études Géologiques et Archéologiques Les Chercheurs de la Wallonie, hours-séire, 4 & Étude et Recherches Archéologiques de l'Université de Liège, 128, pp. 323-334.

Bonjean, D., Abrams, G., Di Modica, K., Otte, M., Pirson, S., Toussaint, M., 2014. Scladina Cave: Archaeological context and history of the discoveries. In: Toussaint, M., Bonjean, D. (Eds.), The Scladina 1-4A Juvenile Neandertal (Andenne, Belgium) Palaeoanthropology and Context, vol. 134. Etude at Recherches Archéologiques de l'Université de Liège. 31-48.

Bookstein, F. L. 1989. 'Size and shape': A comment on semantics. Systematic Zoology, 38, 173–180.

Bookstein F. L. 1991. Morphometric tools for landmark data: geometry and biology. Cambridge University Press, Cambridge (UK); New York.

Böse, M., Lüthgens, C., Lee, J.R., Rose, J. 2012. Quaternary Glaciations of northern Europe. Quaternary Science Reviews 44, 1-25.

de Carlis, A., Alluvione, E., Fonte, A., Rossi, M., Santi, G. 2005: Morphometry of the *Ursus spelaeus* remains from Valstrona (northern Italy). Geo Alp 2, 115–126.

Charters, D., Abrams, G., De Groote, I., Di Modica, K., Bonjean, D., Meloro, C., 2019. Temporal variation in cave bear (*Ursus spelaeus*) dentition: The stratigraphic sequence of Scladina Cave, Belgium. Quaternary Science Reviews .205. 76-85.

Christiansen, P., 2007. Evolutionary implications of bite mechanics and feeding ecology in bears. Journal of Zoology. 272, 423-443.

Clark, P. U., Dyke, A. S., Shakun, J. D., Carlson, A. E., Clark, E., Wohlfarth, B., Mitrovica, X. J., Hostetler, S. W., Mccabe, A. M. 2009. The Last Glacial Maximum. Science (New York, NY) 325:710–714. doi:10.1126/science.1172873.

Clauss, M., Dittmann, M. T., Müller, D. W. H., Meloro, C., Codron, D. 2013. Bergmann's rule in mammals: a cross-species interspecific pattern. Oikos 122: 1465–1472.

Collyer, M. L., Adams, D. C. 2013. Phenotypic trajectory analysis: comparison of shape change patterns in evolution and ecology. Hystrix, It. J. Mamm. 24(1): 75–83

Collyer, M. L., Adams, D. C. 2018. RRPP: RRPP: An R package for fitting linear models to high-dimensional data using residual randomization. Methods in Ecology and Evolution. 9(2): 1772-1779. https://besjournals.onlinelibrary.wiley.com/doi/10.1111/2041-210X.13029

Collyer, M. L., Adams, D. C. 2019. RRPP: Linear Model Evaluation with Randomized Residuals in a Permutation Procedure. https://CRAN.R-project.org/package=RRPP

Collyer, M. L., Adams, D. C. 2021. RRPP: Linear Model Evaluation with Randomized Residuals in a Permutation Procedure. https://cran.r-project.org/web/packages/RRPP

Cooper, A., Turney, C., Hughen, K. A., Brook, B. W., McDonald, H. G., Bradshaw, C. J. 2015. Abrupt warming events drove Late Pleistocene Holarctic megafaunal turnover. Science 349:602–606. doi:10.1126/science.aac4315

Dansgaard, W., Clausen, H.B., Gundestrup, N., Hammer, C.U., Johnsen, S.J., Kristinsdottir, P.M., Reeh, N., 1982. A new Greenland deep ice core. Science 218, 1273-1277.

Daura, J., Sanz, M., Allue, E., Vaquero, M., Lopez-García, J. M., Sanchez-Marco, A., Domenech, R., Martinell, J., Carrion, J. S., Ortiz, J. E., Torres, T., Arnold, L. J., Benson, A., Hoffmann, D. L., Skinner, A. R., Julia, R. 2017. Palaeoenvironments of the last Neanderthals in SW Europe (MIS 3): Cova del Coll Verdaguer (Barcelona, NE of Iberian Peninsula). Quaternary Science Reviews. 177 34-56.

Durão, F. D., Jacint Ventura, J., Muñoz-Muñoz, F. 2019. Comparative post-weaning ontogeny of the mandible in fossorial and semi-aquatic water voles. Mammalian Biology. 10.1016.

Elton, S. 2006. Forty years on and still going strong: the use of hominin- cercopithecid comparisons in palaeoanthropology. Journal of the Royal Anthropological Institute. 12:19−38.

Figueirido, B., Palmqvist, P., Pérez-Claros, J. A. 2009. Ecomorphological correlates of craniodental variation in bears and paleobiological implications for extinct taxa: an approach based on geometric morphometrics. Journal of Zoology. 277:70–80.

Garcia, N., 2003. Osos y otros carnivoros de la Sierra de Atapuerca. Fundacion Oso de Asturias.

Gower, J. 1975. Generalized Procrustes analysis. Pyschometrika 40: 33–51.

Grandal-d'Anglade, A., Lopez-Gonzalez, F. 2005. On the factors that influence the morphology of the cave bear dentition and a study of the geographical variation in the lower carnassial. Mitt. Komm. Quartärforsch. Österr. Akad. Wiss. 14, 41-52.

Gullentops F., Deblaere C. 1992. Érosion et remplissage de la grotte Scladina. In M. Otte (ed.), Recherches aux grottes de Sclayn, vol. 1: Le Contexte. Études et Recherches Archéologiques de l'Université de Liège. 27: 9–31.

Hammer, Ø., Harper, D. A. T., Ryan, P. D. 2001. PAST: paleontological statistics software package for education and data analysis. Palaeontologia Electronica. 4, 1-9.

Helmens, K. F. 2014. The Last Interglacial - Glacial cycle (MIS 5-2) re-examined based on long proxy records from central and northern Europe. Quaternary Science Reviews 86, 115-143.

Huston, M. A., Wolverton, S. 2011. Regulation of animal size by eNPP, Bergmann's rule, and related phenomena. Ecol. Monogr. 81, 349-405 (2011).

Huysseune, A. 1995. Phenotypic plasticity in the lower pharyngeal jaw dentition of Astatoreochromis alluaudi (*Teleostei: Cichlidae*). Archives of Oral Biology. 40, 1005–1014.

Huysseune, A., Sire, J-Y., Witte, P, E. 2009. Evolutionary and developmental origins of the vertebrate dentition. Journal of Anatomy. 214, 465–476.

Jernvall, J., Thesleff, I. 2012: Tooth shape formation and tooth renewal: evolving with the same signals. Development 139, 3487– 3497.

Johnsen, S. J., Clausen, H. B., Dansgaard, W., Fuhrer, K., Gundestrup, N., Hammer, C. U., Iversen, P., Steffensen, J. P., Jouzel, J., Stauffer, B., 1992. Irregular glacial interstadials recorded in a new Greenland ice core. Nature. 359, 311-313.

Jung, W., Beug, H. J., Dehm, R. 1972. Das Riß/Würm-Interglazial von Zeifen, Landkreis Laufen an der Salzach. *Bayerische Akademie der Wissenschaften, Abhandlungen der Mathematisch-naturwissenschaftlichen Klasse*. **151**, 1-131.

Kavanagh, K. D., Evans, A. R., Jernvall, J. 2007. Predicting evolutionary patterns of mammalian teeth from development. Nature. 449, 427 – 432.

Klingenberg, C. P. 2011. MorphoJ: an integrated software package for geometric morphometrics. *Molecular Ecology Resources* **11:** 353-357.

Klingenberg, C. P. 2013. Visualizations in geometric morphometrics: How to read and how to make graphs showing shape changes. Hystrix. 24(1):15-24

Knapp, M., Rohland, N., Weinstock, J., Baryshnikov, G., Sher, A., Doris, N., Rabeder, G., Pinhasi, R., Schmitt, H., Hoffreiter, M. 2009. Fist DNA sequences of Asian cave bear fossils reveal deep divergences and complex phylogeographic patterns. Molecular Ecology. 18, 1225–1238.

Koch, P. L., Barnosky, A. D. 2006. Late Quaternary extinctions: State of the debate. Annual Review of Ecology, Evolution, and Systematics. 37: 215–250.

Krajcarz, M., Pacher, M., Krajcarz, M. T., Laughlan, L., Rabeder, G., Sabol, M., Wojtal, P., Bocherens, H. 2016: Isotopic variability of cave bears ($d^{15}N$, $d^{13}C$) across Europe during MIS 3. Quaternary Science Reviews. 131, 51–72.

Krause, J., Unger, T., Noçon, A., Malaspinas, A. S., Kolokotronis, S. O., Stiller, M., Soibelzon, L., Spriggs, H., Dear, P. H., Briggs, A. W., Bray, S. C., O'Brien, S. J., Rabeder, G., Matheus, P., Cooper, A., Slatkin, M., Pääbo, S., Hofreiter, M. 2008. Mitochondrial genomes reveal an explosive radiation of extinct and extant bears near the miocene-pliocene boundary. BMC Evolutionary Biology. 8:-220.

Kurtén, B. 1955. Contribution to the history of a mutation during 1,000,000 years. Evolution 9, 107-118.

Kurtén, B. 1967. Some quantitative approaches to dental microevolution. Journal of Dental Research, 46(5), 817-828.

Kurtén, B. 1968. Pleistocene Mammals of Europe. 317 pp. Weidenfeld and Nicolson, London.

Lister, A.M. 2004. The impact of Quaternary Ice Ages on mammalian evolution. Philosophical Transactions of the Royal Society B 359, 221-241.

Lorenzen, E. D., Nogues-Bravo, D., Orlando, L., Weinstock, J., Binladen, J., Marske, K. A., Ugan, A., Borregaard, M. K., Gilbert, M. T., Nielsen, R., Ho, S. Y., Goebel, T., Graf, K. E., Byers, D., Stenderup, J. T., Rasmussen, M., Campos, P. F., Leonard, J. A., Koepfli, K. P., Froese, D., Zazula, G., Stafford, T. W. Jr., Aaris-Sørensen, K., Batra, P., Haywood, A. M., Singarayer, J. S., Valdes, P. J., Boeskorov, G., Burns, J. A., Davydov, S. P., Haile, J., Jenkins, D. L., Kosintsev, P., Kuznetsova, T., Lai, X., Martin, L. D., McDonald, H. G., Mol, D., Meldgaard, M., Munch, K., Stephan, E., Sablin, M., Sommer, R. S., Sipko, T., Scott, E., Suchard, M. A., Tikhonov, A., Willerslev, R., Wayne, R. K., Cooper, A., Hofreiter, M., Sher, A., Shapiro, B., Rahbek, C., Willerslev, E. 2011. Species-specific responses of Late Quaternary megafauna to climate and humans. Nature. 2;479(7373):359-64.

Martinez, C. M., McGee, M. D., Borstein, S. R., Wainwright, P. C. 2018. Feeding ecology underlies the evolution of cichlid jaw mobility. Evolution. 72, 8, 1645-1655.

Mattson, D.J. 1998. Diet and morphology of extant and recently extinct northern bears. Ursus. 10, 479-496.

Meiri, S., Dayan, T. 2003. On the validity of Bergmann's rule. Journal of Biogeography 30:331–351.

Meiri, S., Thomas, G. H. 2007. The geography of body size challenges of the interspecific approach. Global Ecology and Biogeography 16:689–693.

Meiri, S., Dayan, T., Simberloff, D. 2004. Carnivores, biases and Bergmann's rule. Biological Journal of the Linnean Society. 81: 579–588.

Meiri, S., Yom-Tov, Y., Geffen, E. 2007. What determines conformity to Bergmann's rule? Global Ecology and Biogeography. 16: 788–794.

Meloro, C. 2011. Feeding habits of Plio-Pleistocene large carnivores as revealed by the mandibular geometry. Journal of Vertebrate Paleontology, 31, 428–446.

Meloro, C., Marques de Oliveira A. 2019. Elbow Joint Geometry in Bears (Ursidae, Carnivora): a Tool to Infer Paleobiology and Functional Adaptations of Quaternary Fossils. Journal of Mammal Evolution. 26:133–146.

Meloro, C., Elton, S., Louys, J., Bishop, L. C., Ditchfield, P. 2013 Cats in the forest: predicting habitat adaptations from humerus morphometry in extant and fossil Felidae (Carnivora). Paleobiology 39:323−344.

Meloro, C., Guidarelli, G., Colangelo, P., Ciucci, P., Loy, A. 2017. Mandible size and shape in extant Ursidae (Carnivora, Mammalia): A tool for taxonomy and ecogeography. Journal of Zoological Systematics and Evolutionary Research. 55: 269– 287.

Miracle, P.T., 2011. Sex and size of the Krapina cave bears. In: Toskan, B. (Ed.), Fragments of Ice Age Environments. Proceedings in Honour of Ivan Turk's Jubilee, vol. 21. Opera Instituti Archaeologici Sloveniae, Ljubljana, pp. 85-111.

Mondanaro, A., Di Febbraro, M., Melchionna, M., Carotenuto, F., Castiglione, S., Serio, C., Danisi, S., Rook, L., Diniz-Filho, J. A. F., Raia, P. 2019. Additive effects of climate change and human hunting explain population decline and extinction in cave bears. Boreas. Vol. 48, pp. 605–615. https://doi.org/10.1111/bor.12380. ISSN 0300-9483.

Mori, T., Harvati, K. 2019. Basicranial ontogeny comparison in *Pan troglodytes* and *Homo sapiens* and its use for developmental stage definition of KNM-ER 42700. American Journal of Physical Anthropology. 170:579–594.

Münzel, S. C., Hofreiter, M., Stiller, M., Mittnik, A., Conard, N. J., Bocherens, H. 2011. Pleistocene bears in the Swabian Jura (Germany): genetic replacement, ecological displacement, extinctions and survival. Quaternary International. 245:225–237.

Pappa, S., Schreve, D. C., Rivals, F. 2019. The bear necessities: A new dental microwear database for the interpretation of palaeodiet in fossil Ursidae. Palaeogeography, Palaeoclimatology, Palaeoecology. 514, 168-188.

Peigné. S., Goillot, C., Germonpré, M., Blondel, C., Bignon, O., Merceron, G. 2009. Predormancy diet of the European cave bear: evidence for omnivory from a dental microwear analysis of Late Pleistocene *Ursus spelaeus* from Goyet, Belgium. Proceedings of the National Academy of Sciences of the United States of America. 106(48):15390–15393.

Pérez-Ramos, A., Kupczik, K., Van Heteren, A. H., Rabeder, G., Grandal-D'Anglade, A., Pastor, F. J., Serrano, F. J., Figueirido, B. 2019 A three-dimensional analysis of tooth-root morphology in living bears and implications for feeding behaviour in the extinct cave bear. Historical Biology. 31:4, 461-473.

Pérez-Ramos, A., Tseng, Z. J., Grandal-D'Anglade, A., Rabeder, G., Pastor, F. J., Figueirido, B. 2020. Biomechanical simulations reveal a trade-off between adaptation to glacial climate and dietary niche versatility in European cave bears. Sci. Adv. 6, eaay9462.

Pirson, S., 2007. Contribution à l'étude des dépôts d'entrée de grotte en Belgique au Pléistocène supérieur. Unpublished PhD thesis. In: Stratigraphie, sédimentogenèse et paléoenvironnement, vol. 2. University of Liège and Royal Belgian Institute of Natural Sciences, p. 435. 5 annexes.

Pirson, S., Court-Picon, M., Damblon, F., Balescu, S., Bonjean, D., Haesaerts, P. 2014. The Palaeoenvironmental context and chronostratigraphic framework of the Scladina Cave sedimentary sequence (Units 5 to 3-SUP). In: Toussaint, M., Bonjean, D. (Eds.), The Scladina I-4A Juvenile Neandertal (Andenne, Belgium), Palaeoanthropology and Context, vol. 134. ERAUL, pp. 69-92.

Pirson, S., Court-Picon, M., Haesaerts, P., Bonjean, D., Damblon, F. 2008. New data on geology, anthracology and palynology from the Scladina Cave Pleistocene sequence: preliminary results. In: Damblon, F., Pirson, S., Gerrienne, P. (Eds.), Hautrage (Lower Cretaceous) and Sclayn (Upper Pleistocene). Field Trip Guidebook. Charcoal and Microcharcoal: Continental and Marine Records. IVth International Meeting of Anthracology, Brussels, Royal Belgian Institute of Natural Sciences, 8-13 September 2008, vol. 55. Royal Belgian Institute of Natural Sciences, Memoirs of the Geological Survey of Belgium, Brussels, pp. 71-93.

Peltier, W. R., Fairbanks, R. G. 2006. Global glacial ice volume and Last Glacial Maximum duration from an extended Barbados Sea level record. Quaternary Science Reviews. 25:3322–3337. doi:10.1016/j.quascirev.2006.04.010

Polly, P.D. 2007. Development with a bite. Nature, 449(7161), pp.413-414.

Quinif, Y., Genty D., Maire R. 1994. Les spéléothèmes: un outil performant pour les études paléoclimatiques. Bulletin de la Société géologique de France, 165: 603–612.

R Core Team, 2021. R: A language and environment for statistical computing. R Foundation for Statistical Computing, Vienna, Austria. URL https://www.R-project.org/.

Rabeder, G. 1999. Die Evolution des Höhlenbärengebisses. Mitteilungen der Kommission für Quartärforschung der Osterreichischen Äkademie der Wissenschaften. 11, 1–102.

Rabeder, G., Tsoukala, E. 1990. Morphodynamic analysis of some cave-bear teeth from Petralona cave (Chalkidiki, North-Greece). Beiträge zur Paläontologie Osterreich. 16, 103–109.

Rabeder, G., Debeljak, I., Hofreiter, M., Withalm, G. 2008. Morphological response of cave bears (*Ursus spelaeus* group) to high-alpine habitats. Hohle. 59, 59-70.

Rabeder, G., Pacher, M., Withalm, G. 2010. Early Pleistocene bear remains from Deutsch-Altenburg (Lower Austria). Mitteilungen der Kommission für Quartärforschung der Österreichischen Akademie der Wissenschaften. 17, 1–135.

Rabeder, G., Hofreiter, M., Stiller, M. 2011. Chronological and systematic position of cave bear fauna from Ajdovska jama near Krsko (Slovenia). Mitteilungen der Kommission für Quartärforschung der Osterreichischen Akademie der Wissenschaften 20, 43–50.

Raia, P., Passaro, F., Fulgione, D. & Carotenuto, F. 2012. Habitat tracking, stasis and survival in Neogene large mammals. Biol. Lett. 8, 64-66.

Rasmussen, S. O., Bigler, M., Blockley, S. P., Blunier, T., Buchardt, S. L., Clausen, H. B., Cvijanovic, I., Dahl-Jensen, D., Johnsen, S. J., Fischer, H., Gkinis, V., Guillevic, M., Hoek, W. Z., Lowe, J. J., Pedro, J. B., Popp, T., Seierstad, I. K., Steffensen, J. P., Svensson, A. M., Vallelonga, P., Vinther, B. M., Walker, M. J. C., Wheatley, J. J., Winstrup, M. 2014. A stratigraphic framework for abrupt climatic changes during the Last Glacial period based on three synchronized Greenland ice-core records: refining and extending the INTIMATE event stratigraphy. Quaternary Science Reviews 106, 14-28.

Renvoisé, E., Evans, A. R., Jebrane, A., Labruère, C., Laffont, R., Montuire, S. 2009. Evolution of mammal tooth patterns: new insights from a developmental prediction model. Evolution 63, 1327– 1340.

Richards, M. P., Pacher, M., Stiller, M., Quilés, J., Hofreiter, M., Constantin, S., Zilhão, J., Trinkaus, E., 2008. Isotopic evidence for omnivory among European cave bears: late Pleistocene Ursus spelaeus from the Peştera cu Oase, Romania. Proc Natl Acad Sci U S A 105:600– 604. doi:10.1073/pnas.0711063105

Robu, M. 2016. Age re-assessment of the cave bear assemblage from Ursilor Cave, north-western Romania. International Journal of Speleology. 45, 123–133.

Robu, M., Fortin, J. K., Richards, M. P., Schwartz, C. C., Wynn, J. G., Robbins, C. T., Trinkaus, E. 2013. Isotopic evidence for dietary flexibility among European Late Pleistocene cave bears (Ursus spelaeus). Canadian Journal of Zoology. 91:227–234.

Robu, M., Wynn, J. G., Mirea, I. C., Petculescu, A., Kenesz, M., Puscas, C. M., Vlaicu, M., Trinkaus, E., Constantin, S. 2018. The diverse dietary profiles of MIS 3 cave bears from the Romanian Carpathians: insights from stable isotope ($d^{13}C$ and $d^{15}N$) analysis. Palaeontology. 61, 209–219.

Rohlf, F. J. 2000. On the use of shape spaces to compare morphometric methods. Hystrix, Italian Journal of Mammology, 11, 9–25.

Rohlf, F. J. 2004. tpsSpline, thin-plate spline, version 1.20. Department of Ecology and Evolution. State University of New York at Stony Brook.

Rohlf, F.J., 2015. The tps series of software. Hystrix, Italian Journal of Mammology. 26, 9-12.

Rohlf, F.J., Slice, D.E. 1990. Extensions of the Procrustes method for the optimal superimposition of landmarks. Systematic Zoology. 39, 40-59.

Roseman, C. C., Delezene, L. K. 2019. The Inhibitory Cascade Model is Not a Good Predictor of Molar Size Covariation. Evolutionary Biology 46:229-238.

Sacco, T., Van Valkenburgh, B. 2004. Ecomorphological indicators of feeding behaviour in the bears (Carnivora: Ursidae). Journal of Zoology, 263: 41-54

Sandom, C., Faurby, S., Sandel, B., Svenning, J.C., 2014. Global late Quaternary megafauna extinctions linked to humans, not climate change. Proceeds of the Royal Society B. 281, 3254.

Seetah, T. K., Cardini, A., Miracle, P. T. 2012. Can morphospace shed light on cave bear spatial-temporal variation? Population dynamics of *Ursus spelaeus* from Romualdova pećina and Vindija, (Croatia). Journal of Archaeological Science. 39, 500-510.

Stayton, C. T. 2006. Testing hypotheses of convergence with multivariate data: morphological and functional convergence among herbivorous lizards. Evolution 60:824–841.

Stiller, M., Molak, M., Prost, S., Rabeder, G., Baryshnikov, G., Rosendahl, W., Münzel, S., Bocherens, H., Grandal-d'Anglade, A., Hilpert, B., Germonpré, M., Stasyk, O., Pinhasi, R.,

Tintori, A., Rohland, N., Mohandesan, E., Ho, S. Y. W., Hofreiter, M., Knapp, M. 2014. Mitochondrial DNA diversity and evolution of the Pleistocene cave bear complex. Quaternary International. 339–340, 224–231.

Stuart, A. J. 2015. Late Quaternary megafaunal extinctions on the continents: a short review. Geological Journal. 50: 338–363.

Stuart, A. J., Lister, A.M. 2007. Patterns of Late Quaternary megafaunal extinctions in Europe and northern Asia. Courier Forschungsinstitut Senckenberg. 259; 287 – 297.

Taboda, V., Fernándes, M., Grandal d'Anglade, A. 2001. Cave bear's diet: a new hypothesis based on stable isotopes. Cadernos do Laboratorio Xeolóxico de Laxe Coruña 26.

Terhune, C. E., Ritzman, T. B., Robinson, C. A. 2018. Mandibular ramus shape variation and ontogeny in *Homo sapiens* and *Homo neanderthalensis*. Journal of Human Evolution, 10.1016.

Toskan, B. 2007. Metric study of cave bear skulls from Divje babe I. In: Turk, I. (Ed.), Upper Pleistocene Palaeolithic Site in Slovenia. Part I: Geology and Palaeontology. Opera Instituti Archaeologici Sloveniae, vol. 13, pp. 357e367. Ljubljana. 431–439.

Toskan, B., Bona, F. 2012: Body size variability in cave bears from the Southern Alps. In De Grosse Mazzorin, J., Sacc_a, L., Tozzi, C. (eds.): Atti 6° Convegno Nazionale di Archeozoologia, 47–55. Associazione Italiana di Archeo-Zoologia, Lecce.

Toussaint, M., Bonjean, D. 2014. The Scladina I-4A Juvenile Neandertal (Andenne, Belgium). Liège: Palaeoanthropology and Context. Études et Recherches archéologiques de l'Université de Liège.

Toussaint, M., Bonjean, D., Otte, M. 1994. Découverte de fossiles humains du Paléolithique moyen à la grotte Scladina à Andenne. In: Corbiau M-H, Plumier J, éditeurs. Actes de la deuxième Journée d'Archéologie Namuroise Facultés universitaires Notre-Dame de la Paix, Namur, 26 février 1994. Namur: Ministère de la Région wallonne (DGATLP) – FUNDP (Département d'Histoire de l'Art et d'Archéologie); p. 19–33.

Van Heteren, A. H., Figueirido, B. 2019. Diet reconstruction in cave bears from craniodental morphology: past evidences, new results and future directions, Historical Biology. 31:4, 500-509.

Van Heteren, A. H., MacLarnon, A., Rae, T. C., Soligo, C. 2009. Cave bears and their closest living relatives: A 3D geometric morphometrical approach to the functional morphology of the cave bear *Ursus spelaeus*. Acta Carsologica, 47, 33–46.

Van Heteren, A. H., MacLarnon, A., Soligo, C., Rae, T. C. 2014. Functional morphology of the cave bear (*Ursus spelaeus*) cranium: A three-dimensional geometric morphometric analysis. Quaternary International, 339, 209–216.

Van Heteren, A. H., MacLarnon, A., Soligo, C., Rae, T. C. 2016. Functional morphology of the cave bear (*Ursus spelaeus*) mandible: A 3D geometric morphometric analysis. Organisms, Diversity and Evolution, 16, 299–314.

Van Valkenburgh, B. 1988. Trophic Diversity in Past and Present Guilds of Large Predatory Mammals. Paleobiology. 14(2), 155-173.

Watt, C., Mitchell, S., Salewski, V. 2010. Bergmann's rule: a concept cluster? Oikos 119:89–100.

Zhu, D., Ciais, P., Chang, J., Krinner, G., Peng, S., Viovy, N., Peñuelas, J., Zimoy, S. 2018. The large mean body size of mammalian herbivores explains the productivity paradox during the Last Glacial Maximum. Nat. Ecol. Evol. 2018 24 2, 640-649.

Conflict of interest

There are no conflicts of interest.

Highlights

- Lower molar tooth size increases from Marine Isotope Stage 5 – MIS 3.

- M_3 appears less constrained and much more responsive to environmental changes.

- Cave bear lower molar shape changed to process more fibrous plant material.

- Tooth shape is a powerful ecological tool to understand adaptation of cave bears.